ELSEVIER

Catalysis Today 76 (2002) 133–139

CATALYSIS TODAY

www.elsevier.com/locate/cattod

Enhancement of salicylate photodegradation under bias in binary mixtures

Mauricio E. Calvo, Roberto J. Candal, Sara A. Bilmes*

INQUIMAE-DQIAQF, Facultad de Ciencias Exactas y Naturales, Universidad de Buenos Aires, Ciudad Universitaria Pabellón II, C1428EHA Buenos Aires, Argentina

Abstract

The influence of oxalate and methanol on the photodegradation behaviour of salicylate under bias was studied measuring the time evolution of the photocurrent and the concentration in solution. In N_2 saturated electrolytes, the presence of the second component produces an enhancement of salicylate degradation, but the degradation of the added photolyte decreases. In the presence of O_2 or other electron acceptors salicylate photodegradation is faster, and the positive effect of a sacrificial photolyte is minimised.

Keywords: Photocatalysis; Photoelectrochemistry; TiO_2; Salicylate

1. Introduction

Photocatalysis is a recognised advanced oxidation technique (AOT) that is presently used in medium scale installations under solar illumination for water decontamination [1,2]. The heterogeneous photocatalytic detoxification process uses light to photoexcite a semiconductor catalyst, typically TiO_2 (cheap, non-toxic and abundant). When TiO_2 is illuminated with light of $\leq$400 nm, an electron is promoted from the valence band to the conduction band of the semiconducting oxide to give an electron/hole pair. The valence band potential is positive enough to generate oxidising species, either free holes or bound hydroxyl radicals ($-OH^{\bullet}$, $E^0 = 2.8$ V), which attack oxidisable contaminants. The progressive breakage of molecules yields as final mineral products CO_2, H_2O and dilute inorganic acids. The best developed technologies use a suspension of semiconductor particles, typically TiO_2 Degussa P-25, and the separation of the solid once mineralisation of contaminants requires additive processes. Supported semiconductors are the trivial solution to the separation problem. However, photocatalysis with films has some disadvantages in comparison to powders. First, the area exposed to the liquid phase is reduced in 2–3 orders of magnitude. Second, the diffusion boundary conditions change from binary collisions to that of a particle against a wall, and the rate of diffusion may become the limiting step. Consequently, the greater efficiency for the generation of surface radicals decreases even further from the typical values (0.040 for $-OH^{\bullet}$) due to enhanced bulk and surface recombination of electron–hole pairs [3]. The latter can be minimised when the semiconductor is deposited onto a conducting substrate and operates under bias [4–6]. In contrast to slurry reactors in which the reaction rate is limited by the rate of electron transfer to electron acceptors photocatalysis under bias is not limited by this process as

* Corresponding author. Fax: +541-576-3341.
E-mail address: sarabil@qi.fcen.uba.ar (S.A. Bilmes).

0920-5861/02/$ – see front matter
PII: S0920-5861(02)00213-4

electrons are pumped away through the external circuit. Although considerable improvements have been achieved in the last years in the synthesis of TiO_2 and other semiconductors for photocatalysis [7–9] leading to a specific surface area increase up to a factor of 1000, nanometer sized pores in these materials limit the diffusion of reactants to the catalyst. For this reason, the enhancement of the mineralisation rate is well below the increase in the surface area. Another problem commonly found with supported catalysts is the slow desorption of intermediates and by-products that block the surface and inhibits the catalysis.

The general mechanism for the oxidation of carboxylic acids is the discharge of the carboxylate ion followed by decarboxylation of the intermediate radical (Kolbe reaction). The radicals formed can then undergo coupling or disproportionation reactions [10]. Salicylate photodegradation is a model reaction for the oxidation of aromatic carboxylates found in water waste streams [11–13]. This reaction requires the transfer of 28 electrons for complete mineralisation.[1] However, under bias the surface becomes covered by partially oxidised intermediates and/or by insulating polymers probably formed by reaction between chemisorbed radicals and adjacent adsorbates [13,15].

In this work we explore the possibility of enhancement of salicylate degradation by addition of a second molecule that hinders the formation of long lived adsorbed intermediates and by-products. This "sacrificial photolyte" may react with the chemisorbed radicals or may produce a disruption in the connection between adsorbed monomers, thus allowing the renewal of surface sites. On this basis, the photodegradation of salicylate–oxalate and salicylate–methanol binary mixtures onto TiO_2 films prepared by sol–gel route under bias was studied in N_2 and O_2 saturated electrolytes. These films are active photocatalysts for the oxidation of methanol, oxalate and salycilate in photoelectrochemical cells [12,13,16]. The conditions leading to highest enhancement are derived from the simultaneous determination of remnant organic target concentration in solution and the photocurrent measured during the photodegradation process. The photocatalyst used in this work has been previously characterised [17]; it is composed by ca. 10 nm anatase crystals embedded in an amorphous matrix giving grains of 300 ± 50 nm diameter with r.m.s. roughness of 2 ± 0.5 nm. The electronic structure exhibits exponential band tails as well as a narrow band close to the conduction band assigned to defects.

[1] The measured oxidation potential of salycilate ranges from 1.2 to 1.3 V (vs. NHE) [14].

2. Experimental section

2.1. Materials

All reagents were analytical grade and used without further purification. Solutions were made up using distilled water further purified with a Milli-Q system. The base electrolyte was a 0.1 mol dm^{-3} $NaClO_4$ aqueous solution, made by neutralising carbonate free NaOH with perchloric acid solution until pH 3. Solutions of the organic targets were prepared by dissolving appropriate amounts of the reagents in the base electrolyte and adjusting to pH 3.

2.2. Experimental set-up

All the experiments were carried out in a 3.2 cm^3 electrochemical cell provided with a quartz window and connected to a potentiostat with automatic data acquisition. A saturated calomel electrode was used as reference and a 2 cm^2 Pt mesh as a counter electrode. The working electrode was a conductive glass (ITO, Delta Technologies) coated with a 400 nm thick TiO_2 layer, prepared as in Ref. [16]. Briefly, a dialysed sol prepared from hydrolysis in aqueous media of Ti–*n*-butoxide was deposited by spin coating, and the whole assembly was fired at 400 °C for 3 h in air. The surface area exposed to the electrolyte was 0.625 cm^2.

The UV source was a 150 W XBO Osram Xe lamp fitted in a high-collection-efficiency housing, equipped with a 325 nm cutoff filter in order to prevent homogeneous photochemistry (absorption maxima: 296 nm for salycilate; lower than 250 nm for oxalate and methanol). A $CuSO_4$ solution placed between the lamp output and the cell acts as IR filter for minimising heating. The incident spectrum was therefore a continuum with cutoff edges at 325 and 700 nm. The photon flux incident on the electrode was below 0.5 μeinstein s^{-1} to minimise bulk recombination of electron–hole pairs.

2.3. Experimental procedure

Repetitive potential cycles between −0.67 and 0.60 V were run in the dark until a reproducible voltammogram was obtained. The potential was then held at 0.60 V and the electrode illuminated after a delay of 30 s. Photocurrent was recorded during the illumination period. Unless otherwise stated, the irradiation time was 60 min. Once the irradiation was stopped, a potential sweep from 0.60 to −0.67 V in the dark was run to detect the reduction of fairly stable oxidised species formed on the electrode surface by action of light. In what follows these *I*/*E* profiles are called dark voltammograms.

The reproducibility in the photoresponse of the film was checked in the base electrolyte saturated with N_2 with the same procedure, but with 90 s irradiation. In these blank experiments, a steady state photocurrent of 120–150 μA is obtained in 20–30 s. Then, the base electrolyte was replaced by the organic containing solution saturated with nitrogen or oxygen. In the case of methanol containing solutions, losses by evaporation were minimised by purging the solution before the addition of methanol.

The concentration of each organic target (salicylic acid, oxalic acid or methanol) was measured before and after irradiation. Methanol was determined by Head-Space gas chromatography (Shimadzu GC 17A, Fid Detector) using 1-butanol as internal standard. Salicylic acid concentration was determined measuring the absorbance at 296 nm (Hewlett Packard HP 8453 Diode Array). Oxalate concentration was determined by ionic chromatography (Dionex DX-100, Column AS4A). In order to correlate the photolyte concentration decrease with the conversion to CO_2, totally organic carbon (TOC) was determined in some duplicate experiments using a D5000 Shimadzu TOC. Percent of degradation of each photolyte refers to (remnant/initial) mole ratio, whereas percent of mineralisation refers to (remnant/initial) carbon mole ratio, as measured by TOC.

3. Results and discussion

Results obtained for the photocatalytic degradation of each organic target in a single component solution are compiled in Table 1.

Table 1
Results for degradation of oxalate, methanol and salicylate single component solutions after 60 min irradiation of a TiO_2 film biased at 0.6 V[a]

Organic target	C_0 (M)	Q (C)	n_d	n_h	% deg
N_2					
Oxalic	10^{-2}	2.75	1.44×10^{-5}	1.98	45
	10^{-3}	0.445	2.03×10^{-6}	2.27	63
Methanol	0.16	1.81	5.12×10^{-5}	0.37	10
Salicylic	10^{-3}	0.267	∼0[b]	–	∼0
	10^{-4}	0.170	4.8×10^{-8}	36.8	15
O_2					
Oxalic	10^{-2}	1.34	1.12×10^{-5}	1.24	35
	10^{-3}	0.508	2.02×10^{-6}	2.61	63
Salicylic[c]	10^{-3}	0.271	3.60×10^{-7}	7.8	12
	10^{-4}	0.355	1.41×10^{-7}	26.1	47

[a] C_0: initial concentration (mol dm^{-3}); Q: total charge (C); n_d: degraded moles of organic target; n_h: number of holes per degraded molecule ($n_h = Q/n_d F$); % deg: percent of organic target degraded (% deg $= n_d 100/C_0 V$).
[b] Salicylate degradation below our detection limit.
[c] Illumination time: 40 min.

The affinity of salicylate for TiO_2 is high, and direct hole transfer triggers photodegradation. For this molecule, in absence of oxidants or homogeneous reactions, complete mineralisation to CO_2 involves the transfer of 28 holes ($n^*_{SA} = 28$). However, by irradiation of a TiO_2 film polarised at 0.6 V in 10^{-4} M salicylate containing electrolyte under N_2, the number of holes transferred per degraded salycilate molecule, n_h, is higher that 28 (our analytical limitations preclude the determination of n_h for $C_{SA} = 10^{-3}$ M). These high values are assigned to the participation of photogenerated holes in parallel processes, such as cleavage of water or photocorrosion.

Fig. 1 shows that complete mineralisation of degraded salycilate is not achieved as there is a considerable cathodic charge in the voltammogram run after irradiation that is due to the presence of partially oxidised intermediates and/or by-products on the surface [12,13]. Thus, an even more important fraction of photogenerated holes participates in parallel process. The accumulation of intermediates and/or by-products formed in anaerobic atmosphere is more evident for the most concentrate salycilate solution (Fig. 1a). Under O_2 the coverage by these undesirable species is lower (Fig. 1c), putting on evidence their

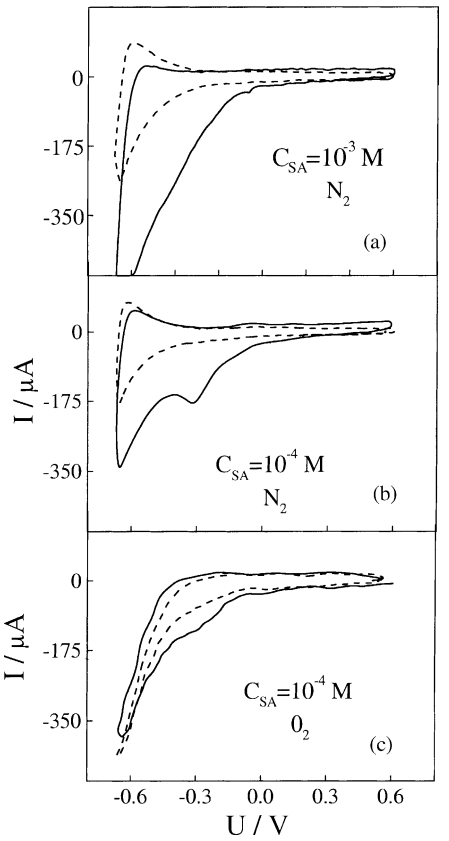

Fig. 1. First cycle of voltammograms run before (- - -) and after (—) 60 min irradiation of salycilate solutions in presence of TiO_2 film electrode biased at 0.6 V, second and subsequent cycles after irradiation are nearly coincident with that recorded before irradiation.

oxidation by O_2. Moreover, dioxygen, and probably other oxidants, participates in homogeneous oxidation steps as deduced from the low values of concentration of remnant salicylate and n_h obtained in O_2 saturated electrolytes (see Table 1). Thus, photodegradation of salycilate under O_2 reduces the requirement of holes (i.e. photons) and the mineralisation pathway is favoured against the formation of chemisorbed intermediates or by-products.

Oxalate exhibits high affinity for the surface, and photodegradation is also initiated by direct hole transfer [13,18]. For this organic target, n_h is close to the value expected for complete mineralisation ($n^*_{OX} = 2$) for $C_{OX} = 0.01$ M, but exceeds n^*_{OX} for the lower initial concentration. For $C_{OX} = 0.001$ M the surface coverage is below saturation [19] thus, parallel process consuming holes occur at the free sites probably via $-OH^\bullet$ radicals. Partially oxidised intermediates or by-products are not detected in the dark voltammogram run after illumination. The other tested component, methanol, has low affinity for the surface. Photodegradation of methanol is initiated by a bimolecular reaction between surface trapped holes as $-OH^\bullet$ and methanol molecules in the vicinity of the surface [12]. The low value of n_h found for methanol ($n^*_{Me} = 4$) is probably due to the high concentration of methanol.

Results obtained for salycilate photoelectrodegradation under N_2, biasing at 0.6 V, in binary mixtures are compiled in Fig. 2. For the sake of comparison data from single component solutions are also plotted. The most important features of these experiments are:

1. For $C_{SA} = 10^{-4}$ M, addition of 10^{-2} M oxalate produces a large increase in the degradation of salicylate.
2. For $C_{SA} = 10^{-3}$ M, the decrease in the mineralisation yield when C_{OX} increases from 10^{-3} to 10^{-2} M suggests the occurrence of opposite effects: at low concentrations, oxalate produces an increase in the salicylate photodegradation rate, whereas at high concentration competition for surface sites is responsible for the low salicylate mineralisation yield.

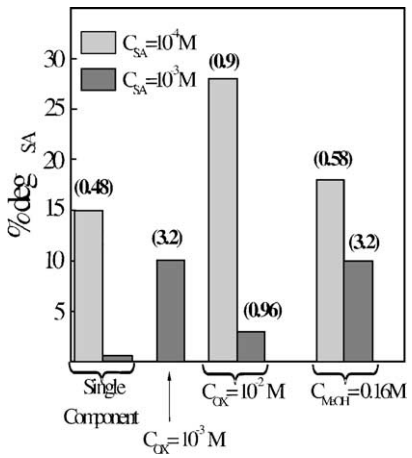

Fig. 2. Amount of degraded salycilate (expressed as % of initial concentration) in solutions with different initial composition. Number in parentheses above each bar correspond to $n_{dSA} \times 10^7$.

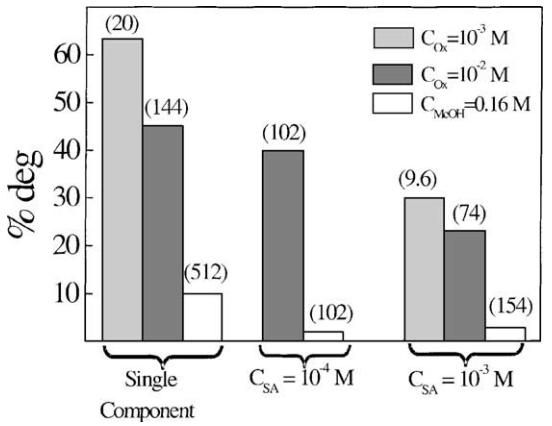

Fig. 3. Amount of degraded oxalate and methanol (expressed as % of initial concentration) in solutions with different initial composition. Number in parentheses above each bar correspond to n_{dMeOH} or $n_{dOX} \times 10^7$. Degradation of single component systems also shown for comparison.

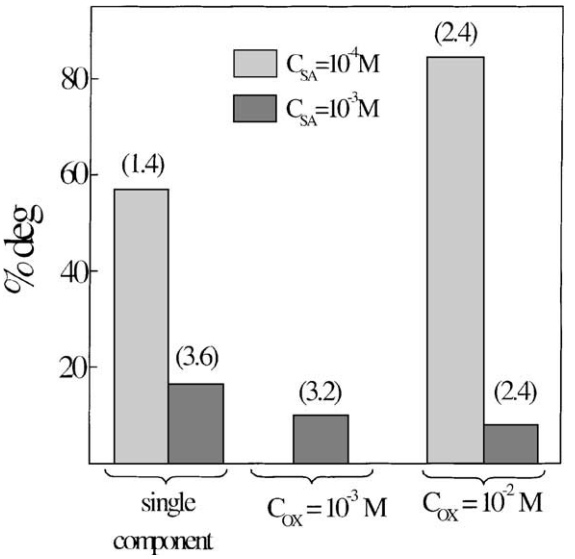

Fig. 4. Amount of degraded salycilate (expressed as % of initial concentration) in oxalate containing solutions under O_2.

3. Addition of methanol produces a modest increase in the photodegradation of 10^{-4} M salicylate solution. For $C_{SA} = 10^{-3}$ M, the enhancement by addition of methanol is comparable to that found for the lowest oxalate concentration. In the case of methanol, other factors should be taken into account, such as homogeneous catalysis, or an increase of salicylate (or its degradation intermediates) solubility in concentrated methanol solutions.

Fig. 3 shows that the presence of salycilate produces a decrease in the degradation of second component. These results reinforce the idea that the competitive adsorption limits the possibility to capture the photogenerated holes; however, salicylate degradation is enhanced by the competing photolyte, even though mineralisation is not fully achieved. Residual TOC in the irradiated solution for $C_{SA} = 10^{-3}$ M and $C_{OX} = 10^{-2}$ M is 7.43×10^{-5} mol C (i.e. 14% mineralisation), lower than the values for salicylate degradation (7.10×10^{-5} mol C, corresponding to 18% degradation); thus, 4% from the initial carbon content (3.3 μmol C) is accounted for partially oxidised intermediates in the liquid phase. The quenching of methanol degradation by salicylate is more important than that of oxalate, indicating that salicylate competes efficiently for $-OH^{\bullet}$. Methanol photodegradation for $C_{SA} = 10^{-4}$ M is lower than for both methanol single component electrolyte and $C_{SA} = 10^{-3}$ M. This rather surprising result may imply that the reaction between adsorbed salicylate and $-OH^{\bullet}$ is more efficient at low salicylate coverages. Indeed, it has been already postulated that depending on the coverage, salicylate gives rise to different intermediate species, some of which, strongly chemisorbed, are able to inject electrons into the conduction band [12].

In O_2 saturated electrolytes the degradation of salicylate in a single component solution is higher than in N_2, and the presence of a second component lead to different trends as shown in Fig. 4. The presence of oxalate leads to a modest increase of salicylate photodegradation for $C_{SA} = 10^{-4}$ M, but has an inhibiting effect for $C_{SA} = 10^{-3}$ M.

A mass balance of the consumed holes shows that the increase in the number of holes used in the enhanced salicylate photodegradation is lower than the decrease in the number used in oxalate or methanol photodegradation. For example, from values of n_d taken from Figs. 2 and 3, the increase of n_{dSA} in the $C_{SA} = 10^{-4}$ M when oxalate is present in $C_{OX} = 10^{-2}$ M would require $28 \times (0.9–0.48) \times 10^{-7} = 12 \times 10^{-7}$ mol of holes for complete mineralisation,[2] whereas from the decrease of n_{dOx} the disponibility

[2] This value may be somewhat higher considering $n_h = 36.8$ found for the single component solution (Table 1).

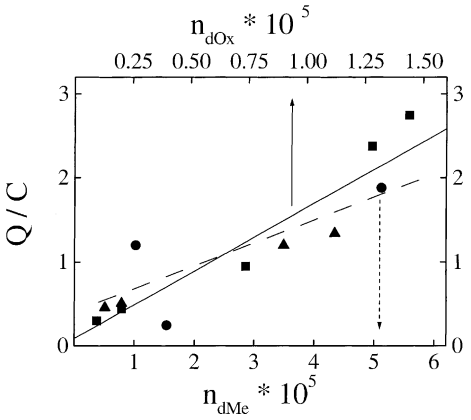

Fig. 5. Charge dependence on degraded methanol (●: lower axis) or oxalate (■: upper axis), measured in experiments with N_2 saturated electrolytes. (▲) Data for oxalate containing solution under O_2.

of holes would increase to $2 \times (144–102) \times 10^{-7} = 84 \times 10^{-7}$ mol. In fact, the charge measured in each experiment with binary mixtures is mostly determined by the photodegradation of oxalate or methanol, as shown in Fig. 5. Data in Fig. 5 exhibit considerable scatter due to the participation of other hole consuming processes (i.e. water oxidation, photocorrosion, as well as changes in the oxidation mechanism leading to different contributions of electron injection into the TiO_2 conduction band). Nevertheless, the slope of linear regression gives average values of $n_h = 0.4$ for methanol and $n_h = 1.7$ for oxalate in agreement with values obtained for the respective single component solutions in Table 1.

Voltammograms recorded after irradiation of the binary mixtures are depicted in Fig. 6. Salicylate partially oxidised intermediates are completely removed for $C_{OX} = 10^{-2}$ M or methanol containing solutions (not shown in the figure), but still persist for $C_{OX} = 10^{-3}$ M. Even if the coverage of partially oxidised intermediates is similar in single component salicylate and in mixtures, the time required to reach this coverage may be longer in the presence of oxalate. In other words, oxalate slows down surface poisoning. On the other side, under O_2, a small amount of adsorbed intermediates is detected in the dark voltammogram run after irradiation for $C_{SA} = 10^{-3}$ M. These chemisorbed species are removed in the presence of oxalate, as seen in Fig. 6b.

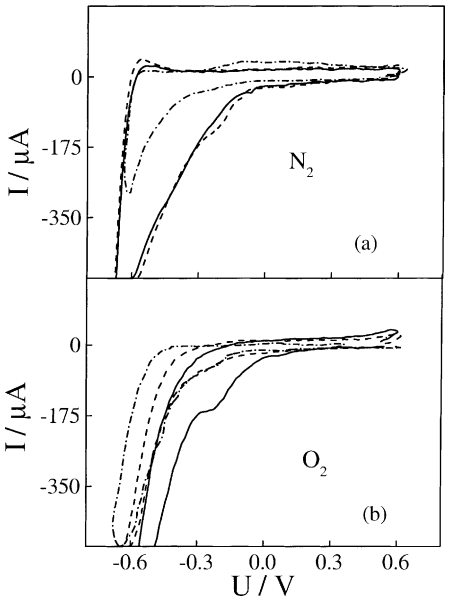

Fig. 6. Voltammograms run after 60 min irradiation at 0.6 V of oxalate–salycilate solutions. (—) $C_{SA} = 10^{-3}$, $C_{OX} = 0$ M; (- - -) $C_{SA} = 10^{-3}$, $C_{OX} = 10^{-3}$ M; (·····) $C_{SA} = 10^{-3}$, $C_{OX} = 10^{-2}$ M. (a) Under N_2; (b) under O_2.

The role of the sacrificial photolyte can be explained with the model of multiple surface sites with different reactivity [13]. Within this picture, adsorbed intermediates or by-products accumulate on sites that contribute little to the overall rate, whereas sites that do not accept intermediates or by-products remain active. However, poisoning may extend to the latter sites, especially if condensation reactions between radicals lead to the growth of polymers on the surface [15].

4. Conclusions

The addition of a “sacrificial photolyte” produces an enhancement in the photodegradation of salicylate, especially in N_2 saturated electrolytes. The most important effect of the second component is the inhibition of steps leading to the accumulation of chemisorbed species that poison the most reactive sites of the surface. Under N_2 the maximum enhancement of salicylate degradation is found when the concentration of both photolytes is below that corresponding to saturation coverage. At high coverages competitive

adsorption and hole transfer minimise the enhancement. In the presence of O_2 or other electron acceptors salicylate photodegradation is faster, and the positive effect of a sacrificial photolyte is minimised.

To achieve an important improvement in the salicylate photodegradation, a considerable amount of the second component has to be added, and longer irradiation times are needed. Nevertheless, this procedure is an interesting alternative to reduce the frequency of thermal treatments required to reactivate supported catalysts, or oxidation–reduction cycles which induce corrosion for semiconductor oxides.

Acknowledgements

This work was supported by research grants from University of Buenos Aires (UBACyT; TX-02/X192) and ANPCyT PICT 4438. We are indebted to Miguel Blesa (UAQ, CNEA, Argentina) for fruitful discussions and for the access to TOC measurements. SAP is a recipient of a René Thalmann-UBA fellowship.

References

[1] D.F. Ollis, H. Al-Ekabi (Eds.), Photocatalytic Purification and Treatment of Water and Air, Elsevier, Amsterdam, 1993.
[2] J. Blanco, S. Malato, Solar Detoxification, UNESCO Engineering Learning Package, 2000, Chapter 7, in press. Available: http://www.unesco.org/science/wsp/publications/solar.htm.
[3] C.J.G. Cornu, A.J. Colussi, M.R. Hoffmann, J. Phys. Chem. B 105 (2001) 1351.
[4] K. Vinodgopal, S. Hotchandani, P.V. Kamat, J. Phys. Chem. 97 (1993) 9040.
[5] D.H. Kim, M.A. Anderson, Environ. Sci. Technol. 28 (1994) 479.
[6] P. Fernandez-Ibañez, S. Malato, O. Enea, Catal. Today 54 (1999) 329.
[7] Q. Xu, M.A. Anderson, J. Mater. Res. 6 (1991) 1073.
[8] S.D. Burnside, V. Shklover, C. Barbe, P. Comte, F. Arendse, K. Brooks, M. Gratzel, Chem. Mater. 10 (1998) 2419.
[9] M. Koelsch, S. Cassaignon, J.-F. Guillemoles, J.-P. Jolivet, Thin Solid Films 312 (2002) 403.
[10] M.N. Baizer, H. Lund, Organic Electrochemistry, Marcel Dekker, New York, 1983.
[11] S. Tunesi, M.A. Anderson, J. Phys. Chem. 95 (1991) 3399.
[12] P. Mandelbaum, S.A. Bilmes, A.E. Regazzoni, M.A. Blesa, Solar Energy 65 (1999) 75.
[13] M.E. Calvo, R.J. Candal, S.A. Bilmes, Environ. Sci. Technol. 35 (2001) 4132.
[14] J. Colucci, V. Montalvo, R. Hernandez, C. Poullet, Electrochim. Acta 44 (1999) 2507.
[15] K. Kratochvilová, I. Hoskovcová, J. Jirkovský, J. Klíma, J. Ludvík, Electrochim. Acta 40 (1995) 2603.
[16] P.A. Mandelbaum, A.E. Regazzoni, M.A. Blesa, S.A. Bilmes, J. Phys. Chem. B 103 (1999) 5505.
[17] S.A. Bilmes, P.A. Mandelbaum, N. Victoria, F. Alvarez, J. Phys. Chem. B 104 (2000) 9851.
[18] J.A. Byrne, B.R. Eggins, J. Electroanal. Chem. 457 (1998) 61.
[19] A.D. Weisz, A.E. Regazzoni, M.A. Blesa, Solid State Ionics 143 (2001) 125.